

RESEARCH LETTER

10.1002/2017GL073219

Key Points:

- A seasonal progression was observed in ^{14}C ages of POC exported from beneath the GrIS
- We propose that patterns result from the seasonal expansion and evolution of the subglacial drainage system
- Future changes in glacial melt may affect downstream productivity via shifts in the bioavailability of carbon

Supporting Information:

- Supporting Information S1

Correspondence to:

T. J. Kohler,
tyler.j.kohler@gmail.com

Citation:

Kohler, T. J., J. D. Žárský, J. C. Yde, G. Lamarche-Gagnon, J. R. Hawkings, A. J. Tedstone, J. L. Wadham, J. E. Box, A. D. Beaton, and M. Stibal (2017), Carbon dating reveals a seasonal progression in the source of particulate organic carbon exported from the Greenland Ice Sheet, *Geophys. Res. Lett.*, *44*, 6209–6217, doi:10.1002/2017GL073219.

Received 23 FEB 2017

Accepted 5 JUN 2017

Accepted article online 9 JUN 2017

Published online 22 JUN 2017

Carbon dating reveals a seasonal progression in the source of particulate organic carbon exported from the Greenland Ice Sheet

T. J. Kohler¹ , J. D. Žárský¹, J. C. Yde², G. Lamarche-Gagnon³, J. R. Hawkings³, A. J. Tedstone³ , J. L. Wadham³, J. E. Box⁴ , A. D. Beaton⁵, and M. Stibal¹ 

¹Department of Ecology, Faculty of Science, Charles University, Prague, Czechia, ²Faculty of Engineering and Science, Western Norway University of Applied Sciences, Sogndal, Norway, ³Bristol Glaciology Centre, School of Geographical Sciences, University of Bristol, Bristol, UK, ⁴Department of Glaciology and Climate, Geological Survey of Denmark and Greenland, Copenhagen, Denmark, ⁵National Oceanography Centre, Southampton, UK

Abstract Surface melt from the Greenland Ice Sheet (GrIS) collects particulate organic carbon (POC) as it drains into subglacial environments and transports it downstream where it serves as a microbial substrate. We hypothesized that older POC is entrained by meltwaters as the subglacial drainage network expands upglacier over the summer. To test this, POC samples were collected from a meltwater river exiting the GrIS over an ablation season and ^{14}C dated. Resulting values were compared with meltwater hydrochemistry and satellite observations of the catchment area. We found that POC ages increased from ~5000 to ~9000 years B.P. until peak discharge and catchment size. Afterward, significant fluctuations in POC age were observed, interpreted to result from periods of high and low subglacial hydrological pressure and sediment supply and subsequent exhaustion. These observations suggest a seasonal progression in the source of POC exported from the GrIS and provide evidence for a seasonally evolving subglacial drainage system.

1. Introduction

Subglacial ecosystems exist between glacial ice and the underlying bedrock and play an important role in storing, transforming, and exporting carbon in one of the fastest-changing habitats on our planet [Hodson *et al.*, 2008]. Glacier and ice sheet beds contain considerable amounts of organic carbon (OC) that was overridden by previous glacial advances [Wadham *et al.*, 2008], and more labile components can be utilized by microbes employing diverse metabolic pathways [Skidmore *et al.*, 2000; Boyd *et al.*, 2010, 2011; Yde *et al.*, 2010; Stibal *et al.*, 2012; Dieser *et al.*, 2014]. In the Arctic, surface meltwater is routed through moulins and crevasses into the subglacial drainage system [Zwally *et al.*, 2002; Copland *et al.*, 2003; Das *et al.*, 2008], where it entrains dissolved and particulate organic carbon (DOC and POC, respectively), eventually exporting them into proglacial streams, lakes, and estuaries [Bhatia *et al.*, 2013; Chandler *et al.*, 2013; Chu, 2014]. Glacially sourced OC has been demonstrated to be bioavailable [Fellman *et al.*, 2010; Lawson *et al.*, 2014b] and to become more so with increasing carbon age [Hood *et al.*, 2009; Singer *et al.*, 2012].

Glaciers contribute an estimated ~0.6% of the total DOC and ~1% of the total POC globally exported by riverine systems to coastal oceans [Hood *et al.*, 2015]. Of this, the Greenland Ice Sheet (GrIS) is the largest source of glacially derived POC (61% of the total glacial flux) [Hood *et al.*, 2015], with POC fluxes more than double that of DOC [Bhatia *et al.*, 2013; Lawson *et al.*, 2014b]. However, these estimates are based on very few samples, likely due to logistical constraints associated with sampling, and as a result, POC is a much neglected component of glacial OC export [Hood *et al.*, 2015]. Recently, Lawson *et al.* [2014b] found POC flushed from Leverett Glacier in West Greenland to be almost exclusively subglacially derived (with all potential supraglacial sources below detection) and to have a considerable labile fraction (~9% carbohydrates). Therefore, achieving a better understanding of the subglacial source of POC, and the seasonal dynamics therein, remains a timely frontier for exploration.

The GrIS subglacial drainage system evolves from an inefficient distributed system to an efficient hydrological network with increasing quantities of supraglacial meltwater input [Chandler *et al.*, 2013]. The hydrology of the subglacial environment has previously demonstrated importance for explaining patterns in downstream meltwater chemistry [Hawkings *et al.*, 2014, 2016; Hindshaw *et al.*, 2014; Yde *et al.*, 2014], as well as sediment and carbon loads [Cowton *et al.*, 2012; Lawson *et al.*, 2014a, 2014b]. Hydrologic perturbations, such as

the drainage of supraglacial lakes to the ice sheet bed, can rapidly flush subglacial water and sediment reservoirs in what are referred to as “outburst” events. As these can be readily identified by observing simultaneous peaks in pH, electric conductivity (EC), suspended sediment, and discharge within a time series [Bartholomew *et al.*, 2011; Hasholt *et al.*, 2013; Hawkings *et al.*, 2016], they represent an opportunity to monitor changes in the subglacial drainage system in a relatively simple and reliable way.

Here we test if the seasonal evolution of the subglacial drainage system corresponds with shifts in the source of exported POC from the GrIS. We measured the ^{14}C age of discrete POC samples taken from the outflow of Leverett Glacier in the western part of the GrIS over a melt season and link our results to the hydrochemical characteristics of the meltwater and changes in the catchment area as monitored by satellite. ^{14}C ages provide a measure of the degree to which POC reservoirs are isolated from each other and the atmosphere and an estimate of the original substrate's age. While this approach has been frequently used to investigate sources of DOC in glacial runoff [e.g., Hood *et al.*, 2009; Singer *et al.*, 2012; Spencer *et al.*, 2014a, 2014b], it has been utilized less frequently for POC [Bhatia *et al.*, 2013]. We hypothesize that older POC is flushed as the subglacial drainage expands into the GrIS over the summer because inland sediments have likely been covered by ice for longer periods of time [Ten Brink and Weidick, 1975; Young and Briner, 2015].

2. Materials and Methods

2.1. Leverett Glacier Hydrology and Water Chemistry

Leverett Glacier (Figure S1 in the supporting information) drains a large ice sheet catchment and was chosen both for its relatively convenient access to the meltwater river draining from its portal (*Akuliarusiarsuup Kuaa*), as well as its recent subglacial research history [e.g., Bartholomew *et al.*, 2010, 2011; Cowton *et al.*, 2012; Hindshaw *et al.*, 2014; Hawkings *et al.*, 2014, 2015]. Discharge, turbidity, pH, and EC were monitored at 15 min intervals in the Leverett Glacier river (Figure S1) over the 2015 summer. The seasonal record includes the onset of summer melt for turbidity, pH, and EC (6 May to 29 July), while discharge was measured from 28 May to the termination of runoff (15 September). Stage was measured by several Hobo® pressure transducers placed at a solid bedrock section of the river ~2 km from the portal (Figure S1). Stage was converted to discharge by creating a rating curve calibrated with Rhodamine dye injections undertaken over the full range of observed river stages [Bartholomew *et al.*, 2011; Cowton *et al.*, 2012]. The turbidity record was used to calculate suspended sediment concentration (SSC), using manually collected depth-integrated samples taken from the water column over a wide range of turbidities as in Bartholomew *et al.* [2011] and Hawkings *et al.* [2014]. Finally, EC was recorded using a Campbell Scientific electrical conductivity and temperature probe (calibrated at a reference temperature of 20°C), and pH was measured continuously using an ion-selective field-effect transistor Honeywell Durafet® pH sensor, as per Hawkings *et al.* [2016].

2.2. POC Collection and Preparation

Suspended sediment samples were taken from the water column near the “cliff” site (N67.064353°, W50.180193°), ~500 m downstream of the Leverett Glacier portal (Figure S1), and processed for POC similarly to Bhatia *et al.* [2013]. Samples were collected at approximately the same time each day (between 10:15 and 12:30, corresponding to the period preceding the diurnal rising limb of the hydrograph), with the exception of those taken on 25 and 27 June, which were sampled at 16:00 and 20:30, respectively (Table S1). Briefly, 5 L of water was collected in cleaned, triple-rinsed glass bottles and transported to the field laboratory where they were kept chilled and in the dark. Suspended sediments were collected onto 0.45 μm Whatman® GF/F filters using a glass filtration tower and promptly frozen in the field freezer (−20°C).

To provide baseline samples, recently exposed subglacial sediment was identified and sampled at the Leverett Glacier terminus (N67.059050°, W50.171400°), as well as the moraine closest to the terminus (N67.060333°, W50.176817°) on 28 July 2015 (Figure S1). Samples were transferred into Whirl-Pak® bags, frozen upon return to the field camp, and stored and transported in the dark. Both moraine and suspended sediment samples were freeze dried, and aliquots were sent to the Laboratory of Ion Beam Physics, Zürich, Switzerland for %C and $\Delta^{14}\text{C}$ analyses. Sediments were liberated from filters following lyophilization and transferred to prepared glass vials; thus, no filter material was included in the analyses. The %C was measured on a vario MICRO Element Analyzer and $\Delta^{14}\text{C}$ analyzed according to Hajdas *et al.* [2004] and Hajdas [2008].

Resulting ^{14}C dates are reported according to *Stuiver and Polach* [1977] as ^{14}C age B.P., and standard deviations for all samples were between 30 and 43 years B.P. (-10.8 and -12.4% ; Table S1).

To compare with POC, water samples were also collected for DOC at approximately the same time each day at the “camp sensors” site, ~ 1 km from Leverett Glacier terminus (Figure S1) using acid-washed 1 L Nalgene™ HDPE bottles thoroughly rinsed with river water. Samples for DOC were immediately filtered through Whatman® Puradisc Aqua 0.45 μm syringe filters and stored frozen (-20°C) in acid-washed 30 mL Nalgene HDPE bottles. DOC was quantified with a Shimadzu TOC-L analyzer. To compare POC with DOC concentrations, we multiplied %C-POC by the corresponding calculated SSC (g L^{-1}) to report POC (in mg L^{-1}), following *Lawson et al.* [2014b]. Discharge-weighted values were calculated for both POC and DOC to estimate their loads (in mg C s^{-1}) and to compare temporal patterns between size fractions.

2.3. MODIS Satellite Observations

To serve as a proxy for the upglacier expansion of the subglacial drainage system (and thus the inland distance that supraglacial melt may enter the ice sheet and access subglacial carbon stores), we quantify transient changes in snowline distances and catchment area (defined as the hydrologically active area draining to the ice sheet margin) over the course of the melt season. The approximate location of the snow-ice transition, or “snowlines,” was extracted in 0.1° latitude bins from samples of 500 m resolution Moderate Resolution Imaging Spectroradiometer (MODIS) MOD10A1 albedo data, processed to remove cloud artifacts [Box *et al.*, 2012]. We used an albedo value of 0.58 to define the break in reflectance between snow and bare ice and present the median longitudinal location of the snow-ice transition for the days on which POC samples were taken. “Snowline distances” are reported as a straight line distance from the portal to the point where the snowline roughly intersects the catchment, and snowline data were then used to calculate catchment size for each sample date, using the catchment area defined in *Palmer et al.* [2011]. For the last sample date (26 July), images were obscured by clouds from 22 to 27 July, and therefore, the snowline is estimated from an image taken on 28 July, which was the nearest cloud-free day.

2.4. Statistical Analyses

To evaluate the hypothesis that POC age increases as the subglacial drainage system extends upglacier, linear regression models were created by including discharge, catchment area, and snowline distance individually as explanatory variables for POC age. Furthermore, we evaluated the coupled/decoupled nature of POC and DOC by regressing corresponding samples against each other (i.e., those taken the same day), as well as by comparing their loads with discharge and catchment characteristics. Adjusted R^2 and p values are reported (with significance designated at $\alpha = 0.05$); all statistical analyses were conducted with the R console, version 3.2.3 [R Core Team, 2015].

3. Results

The early portion of the 2015 melt season was characterized by discharge under $\sim 50 \text{ m}^3 \text{ s}^{-1}$ and diurnal maxima and minima related to Sun angle (Figure 1). Outburst events were observed through changes in hydrochemical properties of the proglacial river. Discharge, pH, EC, and turbidity began to rise near 19 June, leading up to the first subglacial outburst event (Figure 1). Three more outbursts were discerned over the course of the summer melt season near 25 June, 1 July, and 9 July (Figure 1). The peak seasonal discharge of $368 \text{ m}^3 \text{ s}^{-1}$ was observed on 9 July, while the peak in suspended sediment load (495 kg s^{-1}) took place on 3 July, closely followed by another peak on 10 July (Figure 1). The first six POC samples were taken during the “outburst period” (i.e., the seasonal period encompassing all observed outburst events from 19 June to 11 July) and correspond with the rising limbs of each of the four outbursts. Following this seasonal peak in discharge, both discharge and suspended sediment load decreased and diurnal patterns intensified for the remainder of the monitored melt season. There were no further outburst events identified after this point, and the last four POC samples were taken during this “postoutburst” period.

Calculated snowline distances ($n = 10$, $R^2 = 0.639$, and $p = 0.003$) and catchment areas ($n = 10$, $R^2 = 0.522$, and $p = 0.011$) increased over the summer. By 10 July, the retreating snowline had exposed 87% of the total hypothesized surface catchment area (1017 of 1173 km^2), and both snowline distances and catchment areas began to plateau. On 21 July, the snowline had surpassed the entire catchment area (Figure 2) and was

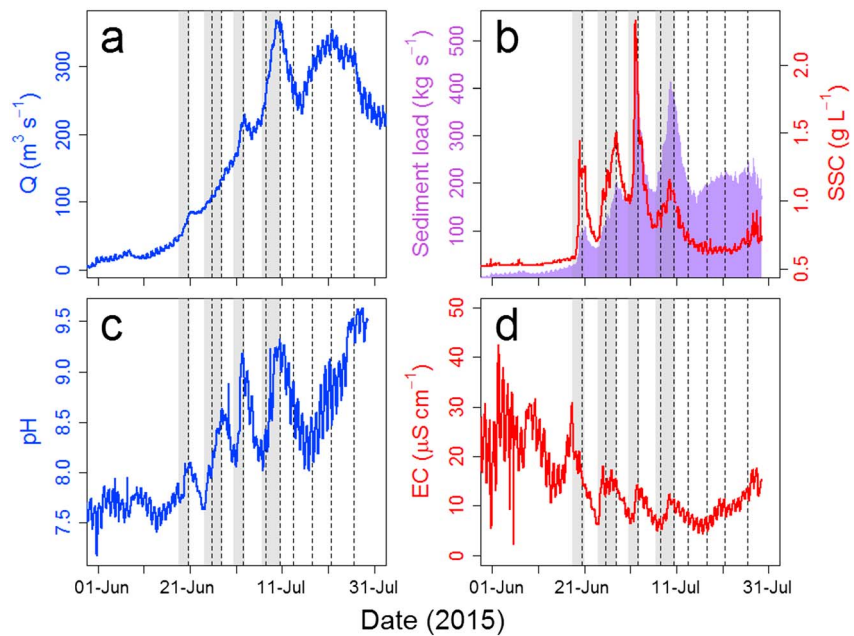


Figure 1. Time series of (a) discharge, (b) suspended sediment concentration (right y axis) and load (left y axis), (c) pH, and (d) conductivity over the 2015 summer. Rising limbs of outburst events are indicated as vertical grey bars. POC sampling time points are indicated as dotted vertical lines.

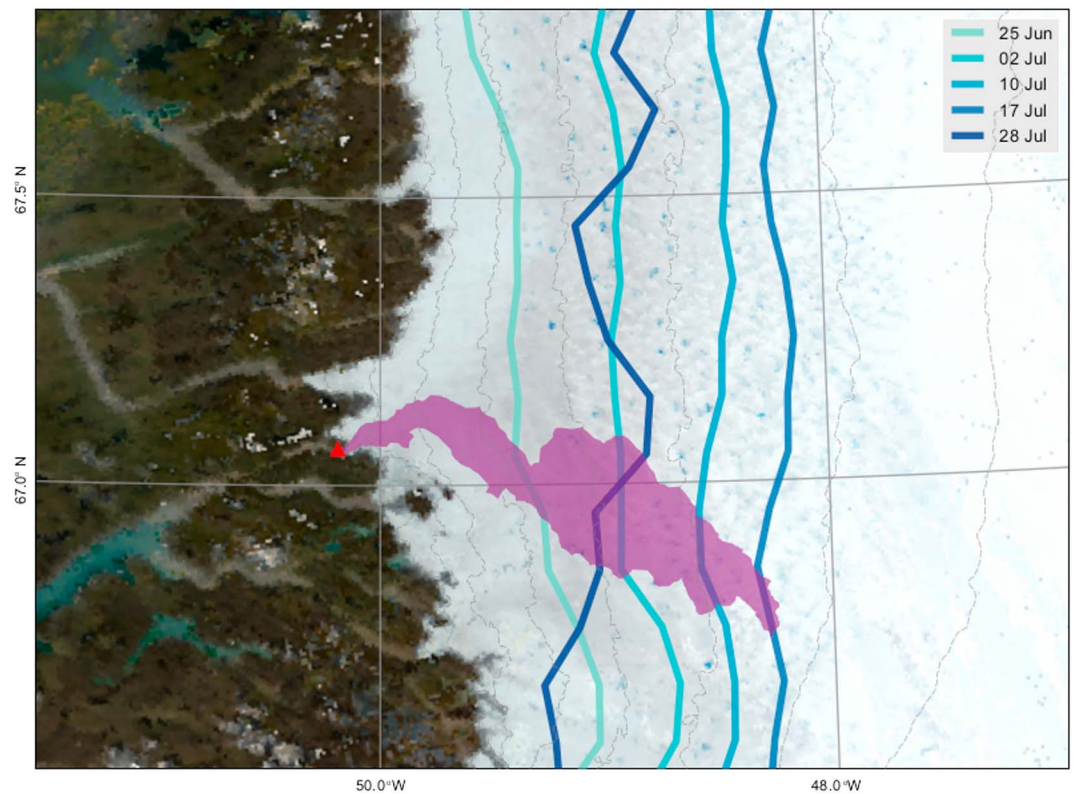


Figure 2. Map of the satellite-inferred snowline corresponding with POC sample dates for the 2015 melt season. Background: MODIS true color image derived from the MOD09GA surface reflectance product, acquired on 10 July 2015. Lines indicate every other sampling date, with the exception of the last date (28 July), as indicated in methods. Portal is indicated as a red triangle, and catchment (purple) is estimated from *Palmer et al.* [2011].

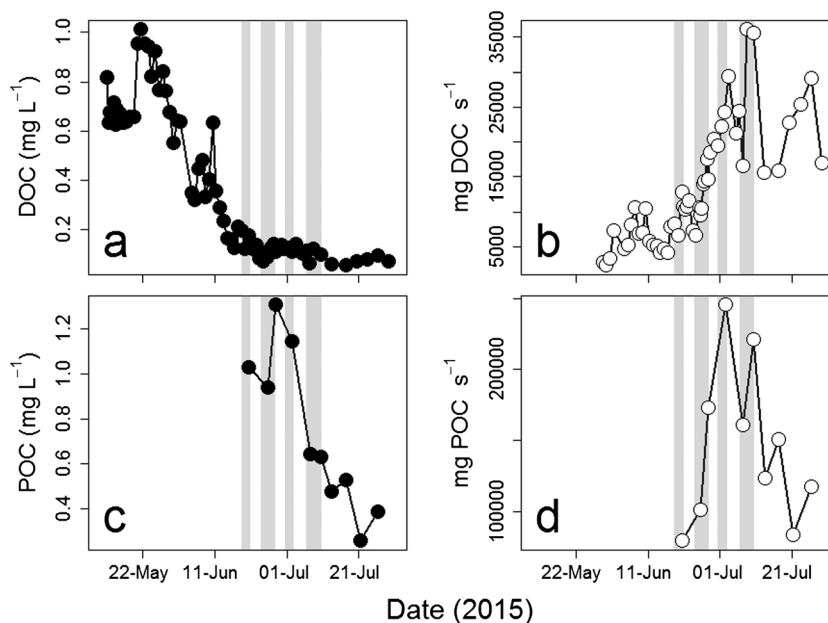


Figure 3. Time series of (a) dissolved organic carbon (DOC) concentration, (b) DOC load, (c) particulate organic carbon (POC) concentration, and (d) POC load for the 2015 summer. Rising limbs of outburst events are indicated as vertical grey bars.

~90 km from the glacier margin (Table S1). After this time, clouds settled into the area and prevented satellite acquisitions. When the clouds lifted on 28 July, the snowline had readvanced substantially (from 89 to 60 km from the margin), reducing the catchment size to the area last observed 2 July and measuring roughly half the full catchment extent (Figure 2 and Table S1).

The percentage of organic carbon (POC) in suspended sediment was between 0.038 and 0.092%, with an average of 0.069% (Table S1), in the range reported by *Lawson et al.* [2014b]. The values were greater than those measured for terminus (0.031%) and moraine (0.036%) sediments. Concentrations of DOC in the meltwater ranged between 0.056 and 1.01 mg L⁻¹, with an average of 0.380 mg L⁻¹, and declined over the course of the melt season (Figure 3). POC concentrations also declined over the summer and ranged between 0.256 and 1.31 mg L⁻¹, averaging 0.734 mg L⁻¹ (Figure 3). When corrected for discharge, DOC loads ranged from 2.3 to 36 g DOC s⁻¹ and averaged 13 g DOC s⁻¹ (Figure 3). POC loads were almost an order of magnitude greater than DOC and ranged from 79 to 245 g POC s⁻¹, with an average of 146 g POC s⁻¹ (Figure 3). There was no significant relationship between POC and DOC loads. Furthermore, while DOC load was positively correlated with discharge ($n = 10$, $R^2 = 0.523$, and $p = 0.011$), there was no significant relationship between POC load and discharge. Neither DOC nor POC was significantly related to catchment size or snowline distance.

The lower range of POC ages exported from the Leverett Glacier meltwater stream was comparable to the bulk material from the Leverett Glacier terminus (4929 years B.P.; -462.4‰) and the nearest moraine (4147 years B.P.; -407.5‰ ; Table S1). POC ages increased over the outburst period from ~5000 years B.P. to 10 July (8929 years B.P.; -673.3‰) and during this time was positively correlated with discharge ($n = 6$, $R^2 = 0.75$, and $p = 0.016$), snowline distance ($n = 6$, $R^2 = 0.650$, and $p = 0.033$), and catchment size ($n = 6$, $R^2 = 0.727$, and $p = 0.019$). This was followed by the postoutburst period, as indicated by a falling limb of discharge and suspended sediment loads, and POC ages fluctuated widely (between ~4000 and ~8000 years B.P.) for the final four samples (Figure 4). Linear models fitted for the entire POC age data set returned no significant results, and the best correlated variable was discharge ($n = 10$ and $R^2 = 0.14$). However, when the two outlying POC samples from the postoutburst period are removed (i.e., 13 and 21 July), POC age was significantly, positively correlated with snowline distance ($n = 8$, $R^2 = 0.620$, and $p = 0.012$), catchment area ($n = 8$, $R^2 = 0.669$, and $p = 0.008$), and discharge ($n = 8$, $R^2 = 0.797$, and $p = 0.002$).

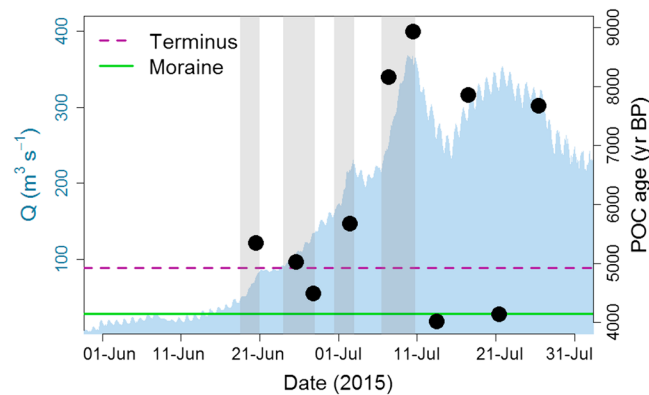


Figure 4. Time series of calculated POC ages (black circles, right y axis) plotted over discharge (filled area, left y axis). Horizontal lines indicate POC ages for Leverett Glacier terminus basal ice (dotted purple) and the first moraine (solid green). Rising limbs of outburst events are indicated as vertical grey bars. Error bars fall within the circular markers, and standard deviations for all samples range from 30 to 43 years B.P.

burst period), and the youngest age we report (~ 4000 years B.P.) came directly after the oldest (measured during the final outburst event), and wide fluctuations in POC ages were observed for these final four samples. We interpret these observations to collectively result from two dynamic, interacting mechanisms: alternating subglacial hydrologic pressure regimes, coupled with the supply of sediment reservoirs and their stochastic depletion.

During the Holocene Thermal Maximum at 6800 ± 300 years B.P., the ice sheet receded inland from its present-day position [van Tatenhove *et al.*, 1996; Levy *et al.*, 2012]. Hence, the lower range of ^{14}C -POC ages and moraine material corresponds to the minimum extent of the GrIS during the middle to late Holocene ~ 5000 to 3000 years B.P. (4200 – 1800 years B.P. for the Kangerlussuaq region, specifically [Young and Briner, 2015]). The last known interglacial period prior to this time corresponds to the Eemian, $130,000$ to $115,000$ years B.P. [Dahl-Jensen *et al.*, 2013] and should be completely depleted of ^{14}C [Hajdas, 2008]. Therefore, the upper range of our observed POC ages (~ 9000 – 7500 years B.P.) probably reflects the mixing of Eemian and Holocene materials, with greater ages indicative of proportionately greater contributions of ^{14}C -depleted POC. However, the inland distance to which different POC sources correspond remains ambiguous, and the degree of Holocene margin fluctuation in the Kangerlussuaq area itself is debated [Simpson *et al.*, 2009; Young and Briner, 2015]. Furthermore, while we assumed a potential Leverett Glacier river catchment 1173 km^2 in size, previous studies have indicated that only 600 km^2 is necessary to explain discharge [Bartholomew *et al.*, 2011], and the efficient system is only known to extend (at least) $\sim 50 \text{ km}$ inland [Chandler *et al.*, 2013]. Therefore, POC may be sourced from nearer to the margin than suggested by our estimates of catchment areas based on snowline position.

We hypothesize that the observed variability in POC ages reflects varying subglacial hydraulic pressure, which rises transiently whenever the meltwater supply rate increases more quickly than the morphology of the subglacial drainage system can evolve to accommodate it. During outburst events, subglacial hydrological pressure increases as surface waters rapidly drain to the bed [Andrews *et al.*, 2014; Hoffman *et al.*, 2016]. This is likely to result in the flushing of old sediments from the existing inefficient distributed system and from previously isolated areas of the bed which become hydrologically connected. As the season progresses, continuing inputs of meltwater lead to the evolution of a more efficient system [Copland *et al.*, 2003; Chandler *et al.*, 2013; Tedstone *et al.*, 2015]. Sediments and POC will then be evacuated from surrounding hydraulically inefficient areas only when there is a gradient of higher to lower pressure into the efficient areas.

Observations of ice motion made $\sim 18 \text{ km}$ inland from the Leverett Glacier terminus suggest that the hydrologic pressure gradient reverses diurnally [Tedstone *et al.*, 2014], indicating the presence of a variable pressure axis as observed in Alpine glaciers [Hubbard *et al.*, 1995]. Similarly, modelling suggests that pressure

4. Discussion

Here we used ^{14}C dating to evaluate the hypothesis that POC exported from the GrIS gets progressively older as the subglacial drainage system expands, corresponding with shifts in POC source. We observed POC ages to increase throughout the early season (i.e., during the outburst period) as new sediment reservoirs were accessed with increasing discharge, catchment area, and snowline distances and spanned a difference of ~ 5000 years. However, this pattern deteriorated during the second half of the season as the rate of catchment expansion slowed (the postout-

variations in inefficient drainage areas can be forced by a subglacial channel located up to 2 km distant [Werder *et al.*, 2013]. During daytime, elevated pressure forces water out of the efficient system and into the inefficient distributed system. When the rate of water supply declines each night, the pressure gradient reverses, flushing material from the inefficient distributed areas of the bed into the efficient system [Hoffman *et al.*, 2016]. While we do not have sufficient data to assess diurnal variations in POC export, the aforesaid mechanism may plausibly explain the wide range of POC ages observed in the second half of the season.

At the same time, increasingly distant and ancient POC stores can be mobilized as the drainage system expands upglacier. Like in previous studies of OC exported from the GrIS [Bhatia *et al.*, 2013; Lawson *et al.*, 2014b], we found POC and DOC to be decoupled, with DOC loads increasing over the summer and POC loads decreasing during the postoutburst period. This suggests that DOC is derived from both supraglacial and subglacial environments, while a greater proportion of POC is sediment bound and derived from subglacial erosion [Hood *et al.*, 2015]. Suspended sediment transport in glacial rivers has previously been shown to exhibit stochastic dynamics related to supply and exhaustion [Cowton *et al.*, 2012; Lawson *et al.*, 2014b]. As most of the defined catchment area was uncovered with snow by 10 July (i.e., the transition between outburst and postoutburst periods), it is possible that some of these reservoirs became depleted, and only limited “new” POC stores were accessed with further snowline migration. Since younger POC presumably enters the stream at all times due to erosion of the near-marginal bed, variability in POC age during the late season may reflect a constant background supply of POC ~4000 years old (such as on 13 and 21 July), augmented by occasional inputs of older ¹⁴C-depleted material as new reservoirs are periodically accessed (i.e., 17 and 26 July).

5. Conclusions

These results lend support to the notion of variable subglacial hydraulic pressure axes causing spatiotemporal variability in accessed POC reservoirs over the summer, which are also prone to supply exhaustion. Understanding processes related to the source and subsequent export of POC is timely, as increased meltwater from longer melt seasons of greater intensity is anticipated to enhance the coupling between subglacial and supraglacial ecosystems [Hodson *et al.*, 2008] and to be generated further inland and at higher elevations [Howat *et al.*, 2013; Leeson *et al.*, 2015; Poinar *et al.*, 2015; Ignéczki *et al.*, 2016]. The subsequent drainage of inwardly expanded supraglacial lakes may accompany changes in carbon and nutrient export if new areas of the glacial bed can be accessed and may therefore have important implications for heterotrophic microbes in carbon-depleted downstream environments [Lawson *et al.*, 2014a, 2014b; Cameron *et al.*, 2017a, 2017b]. Specifically, if POC increases in bioavailability with ¹⁴C age like glacially derived DOC [Hood *et al.*, 2009; Singer *et al.*, 2012], then tapping these sediment sources in the future may have direct implications for productivity in Greenland coastal waters.

Acknowledgments

We thank Elizabeth Bagshaw, Karen Cameron, Jade Hatton, Matthew Marshall, Jon Telling, and Irka Hajdas for field and laboratory assistance. Comments from two anonymous reviewers greatly improved the manuscript. This research was supported by the Czech Science Foundation Junior grant (GACR 15-17346Y) to M.S. Additional support was provided by the Charles University grant (GAUK 279715) to J.Ž. and the UK Natural Environment Research Council (NERC) DELVE grant (NE/I008845/1) to J.L.W. All data used for statistical analyses are given in Table 1 of the supporting information.

References

- Andrews, L. C., G. A. Catania, M. J. Hoffman, J. D. Gulley, M. P. Lüthi, C. Ryser, R. L. Hawley, and T. A. Neumann (2014), Direct observations of evolving subglacial drainage beneath the Greenland Ice Sheet, *Nature*, *514*(7520), 80–83, doi:10.1038/nature13796.
- Bartholomew, I., P. Nienow, D. Mair, A. Hubbard, M. A. King, and A. Sole (2010), Seasonal evolution of subglacial drainage and acceleration in a Greenland outlet glacier, *Nat. Geosci.*, *3*(6), 408–411, doi:10.1038/ngeo863.
- Bartholomew, I., P. Nienow, A. Sole, D. Mair, T. Cowton, S. Palmer, and J. Wadham (2011), Supraglacial forcing of subglacial drainage in the ablation zone of the Greenland ice sheet, *Geophys. Res. Lett.*, *38*, L08502, doi:10.1029/2011GL047063.
- Bhatia, M. P., S. B. Das, L. Xu, M. A. Charette, J. L. Wadham, and E. B. Kujawinski (2013), Organic carbon export from the Greenland ice sheet, *Geochim. Cosmochim. Acta*, *109*, 329–344, doi:10.1016/j.gca.2013.02.006.
- Box, J. E., X. Fettweis, J. C. Stroeve, M. Tedesco, D. K. Hall, and K. Steffen (2012), Greenland ice sheet albedo feedback: Thermodynamics and atmospheric drivers, *Cryosphere*, *6*, 821–839, doi:10.5194/tc-6-821-2012.
- Boyd, E. S., M. Skidmore, A. C. Mitchell, C. Bakermans, and J. W. Peters (2010), Methanogenesis in subglacial sediments, *Environ. Microbiol. Rep.*, *2*, 685–692, doi:10.1111/j.1758-2229.2010.00162.x.
- Boyd, E. S., R. K. Lange, A. C. Mitchell, J. R. Havig, T. L. Hamilton, M. J. Lafrenière, E. L. Shock, J. W. Peters, and M. Skidmore (2011), Diversity, abundance, and potential activity of nitrifying and nitrate-reducing microbial assemblages in a subglacial ecosystem, *Appl. Environ. Microbiol.*, *77*, 4778–4787, doi:10.1128/AEM.00376-11.
- Cameron, K. A., M. Stibal, J. R. Hawkings, A. B. Mikkelsen, J. Telling, T. J. Kohler, E. Gözdereliler, J. D. Zarsky, J. L. Wadham, and C. S. Jacobsen (2017a), Meltwater export of prokaryotic cells from the Greenland ice sheet, *Environ. Microbiol.*, *19*(2), 524–534, doi:10.1111/1462-2920.13483.
- Cameron, K. A., M. Stibal, N. S. Olsen, A. B. Mikkelsen, B. Elberling, and C. S. Jacobsen (2017b), Potential activity of subglacial microbiota transported to anoxic river delta sediments, *Microb. Ecol.*, *74*, 6–9, doi:10.1007/s00248-016-0926-2.
- Chandler, D. M., et al. (2013), Evolution of the subglacial drainage system beneath the Greenland Ice Sheet revealed by tracers, *Nat. Geosci.*, *6*(3), 195–198, doi:10.1038/ngeo1737.

- Chu, V. W. (2014), Greenland ice sheet hydrology: A review, *Prog. Phys. Geogr.*, *38*(1), 19–54, doi:10.1177/0309133313507075.
- Copland, L., M. J. Sharp, and P. W. Nienow (2003), Links between short-term velocity variations and the subglacial hydrology of a predominantly cold polythermal glacier, *J. Glaciol.*, *49*(166), 337–348, doi:10.3189/172756503781830656.
- R Core Team (2015), *R: A Language and Environment for Statistical Computing*, R Foundation for Statistical Computing, Vienna, Austria. [Available at <http://www.R-project.org/>]
- Cowton, T., P. Nienow, I. Bartholomew, A. Sole, and D. Mair (2012), Rapid erosion beneath the Greenland ice sheet, *Geology*, *40*(4), 343–346, doi:10.1130/G32687.1.
- Dahl-Jensen, D., et al. (2013), Eemian interglacial reconstructed from a Greenland folded ice core, *Nature*, *493*(7433), 489–494, doi:10.1038/nature11789.
- Das, S. B., I. Joughin, M. D. Behn, I. M. Howat, M. A. King, D. Lizarralde, and M. P. Bhatia (2008), Fracture propagation to the base of the Greenland Ice Sheet during supraglacial lake drainage, *Science*, *320*, 778–781, doi:10.1126/science.1153360.
- Dieser, M., E. L. J. E. Broensen, K. A. Cameron, G. M. King, A. Achberger, K. Choquette, B. Hagedorn, R. Sletten, K. Junge, and B. C. Christner (2014), Molecular and biogeochemical evidence for methane cycling beneath the western margin of the Greenland Ice Sheet, *ISME J.*, *8*, 2305–2316, doi:10.1038/ismej.2014.59.
- Fellman, J. B., R. G. Spencer, P. J. Hernes, R. T. Edwards, D. V. D'Amore, and E. Hood (2010), The impact of glacier runoff on the biodegradability and biochemical composition of terrigenous dissolved organic matter in near-shore marine ecosystems, *Mar. Chem.*, *121*(1), 112–122, doi:10.1016/j.marchem.2010.03.009.
- Hajdas, I. (2008), Radiocarbon dating and its applications in Quaternary studies, *Eiszeitalter und Gegenwart Quat Sci J.*, *57*(2), 24.
- Hajdas, I., G. Bonani, J. Thut, G. Leone, R. Pfenninger, and C. Maden (2004), A report on sample preparation at the ETH/PSI AMS facility in Zurich, *Nucl. Instrum. Methods Phys. Res., Sect. B*, *223*, 267–271, doi:10.1016/j.nimb.2004.04.054.
- Hasholt, B., A. B. Mikkelsen, M. H. Nielsen, and M. A. D. Larsen (2013), Observations of runoff and sediment and dissolved loads from the Greenland Ice Sheet at Kangerlussuaq, West Greenland, 2007 to 2010, *Z. Geomorphol.*, *57*(2), 3–27, doi:10.1127/0372-8854/2012/5-00121.
- Hawkings, J., J. Wadham, M. Tranter, J. Telling, E. Bagshaw, A. Beaton, S. L. Simmons, D. Chandler, A. Tedstone, and P. Nienow (2016), The Greenland Ice Sheet as a hot spot of phosphorus weathering and export in the Arctic, *Global Biogeochem. Cycles*, *30*, 191–210, doi:10.1002/2015GB005237.
- Hawkings, J. R., J. L. Wadham, M. Tranter, R. Raiswell, L. G. Benning, P. J. Statham, A. Tedstone, P. Nienow, K. Lee, and J. Telling (2014), Ice sheets as a significant source of highly reactive nanoparticulate iron to the oceans, *Nat. Commun.*, *5*, 3929, doi:10.1038/ncomms4929.
- Hawkings, J. R., et al. (2015), The effect of warming climate on nutrient and solute export from the Greenland Ice Sheet, *Geochem. Perspect. Lett.*, *1*, 94–104, doi:10.7185/geochemlet.1510.
- Hindshaw, R. S., J. Rickli, J. Leuthold, J. Wadham, and B. Bourdon (2014), Identifying weathering sources and processes in an outlet glacier of the Greenland Ice Sheet using Ca and Sr isotope ratios, *Geochim. Cosmochim. Acta*, *145*, 50–71, doi:10.1016/j.gca.2014.09.016.
- Hodson, A., A. M. Anesio, M. Tranter, A. Fountain, M. Osborn, J. Priscu, J. Laybourn-Parry, and B. Sattler (2008), Glacial ecosystems, *Ecol. Monogr.*, *78*(1), 41–67, doi:10.1890/07-0187.1.
- Hoffman, M. J., L. C. Andrews, S. A. Price, G. A. Catania, T. A. Neumann, M. P. Lüthi, J. Gulley, C. Ryser, R. L. Hawley, and B. Morriss (2016), Greenland subglacial drainage evolution regulated by weakly connected regions of the bed, *Nat. Commun.*, *7*, 13903, doi:10.1038/ncomms13903.
- Hood, E., J. Fellman, R. G. Spencer, P. J. Hernes, R. Edwards, D. D'Amore, and D. Scott (2009), Glaciers as a source of ancient and labile organic matter to the marine environment, *Nature*, *462*(7276), 1044–1047, doi:10.1038/nature08580.
- Hood, E., T. J. Battin, J. Fellman, S. O'Neel, and R. G. Spencer (2015), Storage and release of organic carbon from glaciers and ice sheets, *Nat. Geosci.*, *8*(2), 91–96, doi:10.1038/ngeo2331.
- Howat, I. M., S. Peña, J. H. Van Angelen, J. T. M. Lenaerts, and M. R. Van den Broeke (2013), Brief Communication "Expansion of meltwater lakes on the Greenland ice sheet", *Cryosphere*, *7*, 201–204, doi:10.5194/tc-7-201-2013.
- Hubbard, B., M. Sharp, I. Willis, M. Nielsen, and C. Smart (1995), Borehole water-level variations and the structure of the subglacial hydrological system of Haut Glacier d'Arolla, Valais, Switzerland, *J. Glaciol.*, *41*(139), 572–583.
- Ignéczki, Á., A. J. Sole, S. J. Livingstone, A. A. Leeson, X. Fettweis, N. Selmes, N. Gourmelen, and K. Briggs (2016), Northeast sector of the Greenland Ice Sheet to undergo the greatest inland expansion of supraglacial lakes during the 21st century, *Geophys. Res. Lett.*, *43*, 9729–9738, doi:10.1002/2016GL070338.
- Lawson, E. C., M. P. Bhatia, J. L. Wadham, and E. B. Kujawinski (2014a), Continuous summer export of nitrogen-rich organic matter from the Greenland Ice Sheet inferred by ultrahigh resolution mass spectrometry, *Environ. Sci. Technol.*, *48*(24), 14248–14257, doi:10.1021/es501732h.
- Lawson, E. C., J. L. Wadham, M. Tranter, M. Stibal, G. P. Lis, C. E. Butler, J. Laybourn-Parry, P. Nienow, D. Chandler, and P. Dewsbury (2014b), Greenland Ice Sheet exports labile organic carbon to the Arctic oceans, *Biogeosciences*, *11*(14), 4015–4028, doi:10.5194/bg-11-4015-2014.
- Leeson, A. A., A. Shepherd, K. Briggs, I. Howat, X. Fettweis, M. Morlighem, and E. Rignot (2015), Supraglacial lakes on the Greenland ice sheet advance inland under warming climate, *Nat. Clim. Change*, *5*, 51–55, doi:10.1038/nclimate2463.
- Levy, L. B., M. A. Kelly, J. A. Howley, and R. A. Virginia (2012), Age of the Ørkendalen moraines, Kangerlussuaq, Greenland: Constraints on the extent of the southwestern margin of the Greenland Ice Sheet during the Holocene, *Quat. Sci. Rev.*, *52*, 1–5, doi:10.1016/j.quascirev.2012.07.021.
- Palmer, S., A. Shepherd, P. Nienow, and I. Joughin (2011), Seasonal speedup of the Greenland Ice Sheet linked to routing of surface water, *Earth Planet. Sci. Lett.*, *302*, 423–428, doi:10.1016/j.epsl.2010.12.037.
- Poinar, K., I. Joughin, S. B. Das, M. D. Behn, J. Lenaerts, and M. R. Broeke (2015), Limits to future expansion of surface-melt-enhanced ice flow into the interior of western Greenland, *Geophys. Res. Lett.*, *42*, 1800–1807, doi:10.1002/2015GL063192.
- Simpson, M. J. R., G. A. Milne, P. Huybrechts, and A. J. Long (2009), Calibrating a glaciological model of the Greenland ice sheet from the Last Glacial Maximum to present-day using field observations of relative sea level and ice extent, *Quat. Sci. Rev.*, *28*, 1631–1657, doi:10.1016/j.quascirev.2009.03.004.
- Singer, S. A., C. Fasching, L. Wilhelm, J. Niggemann, P. Steier, T. Dittmar, and T. J. Battin (2012), Biogeochemically diverse organic matter in Alpine glaciers and its downstream fate, *Nat. Geosci.*, *5*(10), 710–714, doi:10.1038/ngeo1581.
- Skidmore, M. L., J. M. Foght, and M. J. Sharp (2000), Microbial life beneath a high Arctic glacier, *Appl. Environ. Microbiol.*, *66*(8), 3214–3220, doi:10.1128/AEM.66.8.3214-3220.2000.
- Spencer, R. G., W. Guo, P. A. Raymond, T. Dittmar, E. Hood, J. Fellman, and A. Stubbins (2014a), Source and biolability of ancient dissolved organic matter in glacier and lake ecosystems on the Tibetan Plateau, *Geochim. Cosmochim. Acta*, *142*, 64–74, doi:10.1016/j.gca.2014.08.006.

- Spencer, R. G., A. Vermilyea, J. Fellman, P. Raymond, A. Stubbins, D. Scott, and E. Hood (2014b), Seasonal variability of organic matter composition in an Alaskan glacier outflow: Insights into glacier carbon sources, *Environ. Res. Lett.*, *9*(5), 055005, doi:10.1088/1748-9326/9/5/055005.
- Stibal, M., et al. (2012), Methanogenic potential of Arctic and Antarctic subglacial environments with contrasting organic carbon sources, *Global Change Biol.*, *18*, 3332–3345, doi:10.1111/j.1365-2486.2012.02763.x.
- Stuiver, M., and H. A. Polach (1977), Discussion; reporting of C-14 data, *Radiocarbon*, *19*(3), 355–363, doi:10.1017/S003382200003672.
- van Tatenhove, F. G., J. J. van der Meer, and E. A. Koster (1996), Implications for deglaciation chronology from new AMS age determinations in central West Greenland, *Quat. Res.*, *45*, 245–253, doi:10.1006/qres.1996.0025.
- Tedstone, A. J., P. W. Nienow, N. Gourmelen, and A. J. Sole (2014), Greenland ice sheet annual motion insensitive to spatial variations in subglacial hydraulic structure, *Geophys. Res. Lett.*, *41*, 8910–8917, doi:10.1002/2014GL062386.
- Tedstone, A. J., P. W. Nienow, N. Gourmelen, A. Dehecq, D. Goldberg, and E. Hanna (2015), Decadal slowdown of a land-terminating sector of the Greenland Ice Sheet despite warming, *Nature*, *526*, 692–695, doi:10.1038/nature15722.
- Ten Brink, N. W., and A. Weidick (1975), Holocene history of the Greenland Ice Sheet based on radiocarbon-dated moraines in West Greenland, *Grønlands Geologiske Undersøgelse Bull.*, *114*, 1–44.
- Wadham, J. L., M. Tranter, S. Tulaczyk, and M. Sharp (2008), Subglacial methanogenesis: A potential climatic amplifier?, *Global Biogeochem. Cycles*, *22*, GB2021, doi:10.1029/2007GB002951.
- Werder, M. A., I. J. Hewitt, C. G. Schoof, and G. E. Flowers (2013), Modeling channelized and distributed subglacial drainage in two dimensions, *J. Geophys. Res. Earth Surf.*, *118*, 2140–2158, doi:10.1002/jgrf.20146.
- Yde, J. C., K. W. Finster, R. Raiswell, J. P. Steffensen, J. Heinemeier, J. Olsen, H. P. Gunnlaugsson, and O. B. Nielsen (2010), Basal ice microbiology at the margin of the Greenland ice sheet, *Ann. Glaciol.*, *51*, 71–79, doi:10.3189/172756411795931976.
- Yde, J. C., N. T. Knudsen, B. Hasholt, and A. B. Mikkelsen (2014), Meltwater chemistry and solute export from a Greenland Ice Sheet catchment, Watson River, West Greenland, *J. Hydrol.*, *519*, 2165–2179, doi:10.1016/j.jhydrol.2014.10018.
- Young, N. E., and J. P. Briner (2015), Holocene evolution of the western Greenland Ice Sheet: Assessing geophysical ice-sheet models with geological reconstructions of ice-margin change, *Quat. Sci. Rev.*, *114*, 1–17, doi:10.1016/j.quascirev.2015.01.018.
- Zwally, H. J., W. Abdalati, T. Herring, K. Larson, J. Saba, and K. Steffen (2002), Surface melt-induced acceleration of Greenland ice-sheet flow, *Science*, *297*(5579), 218–222, doi:10.1126/science.1072708.